

## Characterizing $x\text{Ba}(\text{Mg}_{1/3}\text{Ta}_{2/3})\text{O}_3 + (1-x)\text{Ba}(\text{Mg}_{1/3}\text{Nb}_{2/3})\text{O}_3$ microwave ceramics using extended x-ray absorption fine structure method

P.-J. Chang and C.-T. Chia<sup>a)</sup>

*Department of Physics, National Taiwan Normal University, Taipei 116, Taiwan*

I.-N. Lin

*Department of Physics, Tamkang University, Tamsui 251, Taiwan*

J.-F. Lee

*National Synchrotron Radiation Research Center, Hsinchu 300, Taiwan*

C. M. Lin

*Department of Science Education, National Hsin-Chu Teachers College, Hsinchu 300, Taiwan*

K. T. Wu

*Department of Physics, Soochow University, Taipei 111, Taiwan*

(Received 29 September 2005; accepted 5 May 2006; published online 15 June 2006)

The structures of  $\text{TaO}_6$  and  $\text{NbO}_6$  oxygen octahedra in  $x\text{Ba}(\text{Mg}_{1/3}\text{Ta}_{2/3})\text{O}_3 + (1-x)\text{Ba}(\text{Mg}_{1/3}\text{Nb}_{2/3})\text{O}_3$  perovskite ceramics with  $x=0, 0.25, 0.50, 0.75$ , and  $1.0$  were investigated by the extended x-ray absorption fine structure method. The decline in the microwave dielectric constant as  $x$  increases is caused mainly by the decrease of the mean volume of the oxygen octahedra, regardless of the 1:2 ordered structure and the distortion of the oxygen octahedron. The low  $Qf$  values of the  $\text{TaO}_6$  and  $\text{NbO}_6$  mixed samples are caused by not only the degrading of the 1:2 ordered structure but also the distortion of oxygen octahedral cages. © 2006 American Institute of Physics. [DOI: 10.1063/1.2213514]

$A(B'_{1/3}B''_{2/3})\text{O}_3$  1:2 ordered ceramics are well known for their potential applications in microwave communications and their high  $Qf$  value which can be exploited in microwave resonators.<sup>1,2</sup>  $B$ -site ordering and its relationship to microwave properties of the similar ceramics, as revealed by the Raman spectroscopy, infrared spectroscopy, and x-ray diffraction, have attracted substantial attention.<sup>3–13</sup> Recent studies have examined how the microwave properties of  $A(B'_{1/3}B''_{2/3})\text{O}_3$  and phonon vibrations are related,<sup>7–9</sup> indicating that structural characteristics of the  $B'O_6$  oxygen octahedra in  $A(B'_{1/3}B''_{2/3})\text{O}_3$  ceramics are critical to the microwave performance. However, optical measurements, including those obtained by Raman spectroscopy or infrared spectroscopy, yield information that indirectly relates phonon vibrations to the microwave characteristics. The  $B'O_6$  local structure must be directly measured, such as by an extended x-ray absorption fine structure (EXAFS), to support the optical measurements.<sup>14,15</sup> Although the crystalline structure of  $x\text{Ba}(\text{Mg}_{1/3}\text{Ta}_{2/3})\text{O}_3 + (1-x)\text{Ba}(\text{Mg}_{1/3}\text{Nb}_{2/3})\text{O}_3$  [hereafter  $x\text{BMT} + (1-x)\text{BMN}$ ] perovskite can be determined by powder x-ray diffraction, this approach cannot easily resolve the differences between the local surroundings of Ta and Nb core atoms. The interferencelike pattern embedded in the EXAFS spectrum yields quantitative information about the local structure near an absorbing atom with relatively sensitive to structural disorder.<sup>12,13</sup> However, discussion of EXAFS to elucidate the effect of  $B''$  site on the microwave characteristics is rare. This work reports the EXAFS results of the Ta  $L_{\text{III}}$  edge and the Nb  $K$  edge of  $x\text{BMT} + (1-x)\text{BMN}$  ceramics, with  $x=0, 0.25, 0.50, 0.75$ , and  $1.0$ . The

structural factors that directly affect the microwave performance are elucidated.

The microwave dielectric properties of  $x\text{BMT} + (1-x)\text{BMN}$  ceramics were measured by the  $\text{TE}_{011}$  resonant cavity method using an HP 8722 network analyzer, around 6 GHz.<sup>16,17</sup> The dielectric constant declines linearly as the Ta concentration increases; BMN ( $x=0$ ) has the highest dielectric constant of 31.4 and BMT ( $x=1$ ) has the lowest dielectric constant of 23.5. The BMT sample also has the highest  $Qf$  value (141.6 kHz) as expected and the  $Qf$  value of BMN (121.1 kHz) is the second highest. The sample with the lowest  $Qf$  value (33.3 kHz) is that with  $x=0.5$ , primarily because the 1:2 ordered structure is degraded, if the Nb and Ta atoms are assumed to be evenly distributed. However, the  $Qf$  value of the  $x=0.75$  sample (46.3 kHz) is two and a half times smaller than that of the  $x=0.25$  sample (114.3 kHz), although they have similar  $B''$  site ordered structure.

Ta  $L_{\text{III}}$ -edge and Nb  $K$ -edge EXAFS measurements were made in wiggler beamline BL17C and beamline BL01C, respectively, at the National Synchrotron Radiation Research Center of Taiwan. The absorption coefficient  $\mu(E)$ , converted from the fluorescence spectrum of the Ta  $L_{\text{III}}$  edge, was obtained between 9.68 and 10.88 keV.  $\mu(E)$  of Nb  $K$ -edge spectra ranged from 18.7 to 20 keV. The absorption coefficient  $\mu(E)$  raised at the absorption edge agrees with the expected growth and is proportional to the concentration of the absorbing atoms. The EXAFS results were interpreted using the FEFF-8 code which is based on real space full multiple scattering calculations;<sup>18</sup> the structural parameters of  $\text{TaO}_6$  and  $\text{NbO}_6$  can be determined to interpret the microwave dielectric characteristics of  $x\text{BMT} + (1-x)\text{BMN}$ .

Figure 1(a) presents the typical momentum ( $k^3$ ) weighted EXAFS signals of the Ta  $L_{\text{III}}$  edge (9.881 keV) and

<sup>a)</sup> Author to whom correspondence should be addressed; electronic mail: chiac@phy.ntnu.edu.tw

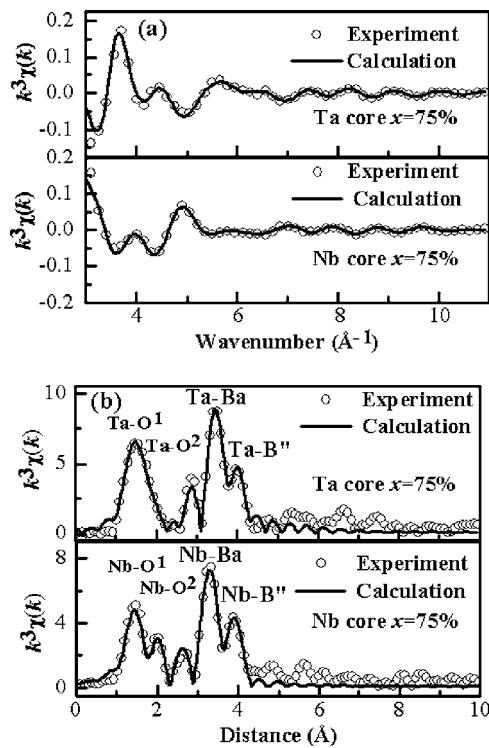


FIG. 1. EXAFS signal of 0.75BMT+0.25BMN. (a)  $k^3$  weighted EXAFS signal of Ta  $L_{III}$  edge and Nb  $K$  edge in  $k$  space and (b) in  $R$  space. Hollow circles represent the experimental data and the solid lines represent the FEFF-8 fitting results.

Nb  $K$  edge (18.986 keV) in momentum ( $k$ ) space for the 0.75BMT+0.25BMN sample after the background was removed using the AUTOBK program in FEFF-8.<sup>18</sup> The  $\chi(k)$  denotes the EXAFS function. Figure 1(b) presents the EXAFS spectra with distance  $R$  measured from the absorbing core atoms at  $B''$  lattice sites. The results presented in Fig. 1(b) were obtained by Fourier transform (FT) of the  $k^3\chi(k)$  EXAFS signals shown in Fig. 1(a). The FTs were performed in the range of 3–11  $\text{\AA}^{-1}$  in  $k$  space. The hollow circles in Fig. 1 represent the experimental results, while the solid lines are the FEFF-8 fitting results. The solid lines in Fig. 1 are the FEFF-8 fitting data for the seven nearest neighboring atoms at 0.9–4.2  $\text{\AA}$  from the core atoms. The FEFF-8 analyses of the other samples are similar to that in Fig. 1, and the  $R$  factors of all fittings were under 0.003. The average distances of the three first nearest oxygen atoms in  $\text{TaO}_6$  (denoted as Ta–O<sup>1</sup>) are around 1.89(4), 1.87(1), 1.85(7), and 1.87(1)  $\text{\AA}$  for  $x=0.25$ ,  $x=0.5$ ,  $x=0.75$ , and BMT samples, respectively, while the Nb–O<sup>1</sup> bonds in  $\text{NbO}_6$  are slightly larger, at around 1.95(6), 1.94(8), 1.94(4), and 1.94(4)  $\text{\AA}$  in the BMN,  $x=0.25$ ,  $x=0.5$ , and  $x=0.75$  samples, respectively. Similarly, the three second nearest three oxygen atoms in  $\text{TaO}_6$ , Ta–O<sup>2</sup>, are around 2.09(0), 2.07(4), 2.07(3), and 2.07(2)  $\text{\AA}$  in the  $x=0.25$ ,  $x=0.5$ ,  $x=0.75$ , and BMT samples, respectively, while those in  $\text{NbO}_6$ , Nb–O<sup>2</sup>, are 2.11(4), 2.11(6), 2.11(8), and 2.12(4)  $\text{\AA}$  for the BMN,  $x=0.25$ ,  $x=0.5$ , and  $x=0.75$  samples, respectively. The EXAFS results indicate that the mean volume of  $\text{NbO}_6$  slightly exceeds that of  $\text{TaO}_6$ , mainly because of the large polarizability of  $\text{Ta}^{5+}$  ions, although the effective ion radii of  $\text{Nb}^{5+}$  and  $\text{Ta}^{5+}$  are about the same.<sup>19–21</sup> However, the polarizability of  $\text{Mg}^{2+}$  is much lower than those of  $\text{Nb}^{5+}$  and  $\text{Ta}^{5+}$ . Therefore, we expect that the microwave dielectric constants of  $x\text{BMT}+(1-x)\text{BMN}$

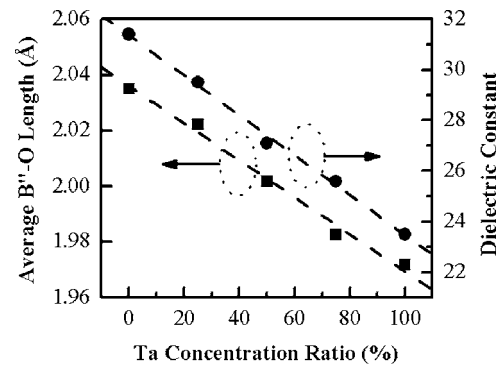


FIG. 2. Plot of the averaged  $B''$ –O bond length, determined using  $[x\text{TaO}^1 + (1-x)\text{NbO}^1 + x\text{TaO}^2 + (1-x)\text{NbO}^2]/2$ , and dielectric constant of  $x\text{BMT} + (1-x)\text{BMN}$  ceramics vs Ta concentration.

are strongly related to the polarizability of the  $B''$ -site ion.

Figure 2 plots the mean length of  $B''$ –O bond in  $B''\text{O}_6$  oxygen octahedra and the dielectric constant of the  $x\text{BMT} + (1-x)\text{BMN}$  ceramics versus Ta concentration ratio  $x$ . The averaged  $B''$ –O bond lengths of  $B''\text{O}_6$  were determined using the formula  $[x\text{TaO}^1 + (1-x)\text{NbO}^1 + x\text{TaO}^2 + (1-x)\text{NbO}^2]/2$ , in which the superscripts 1 and 2 refer to the first and second nearest oxygen atoms in the  $B''\text{O}_6$  octahedra, respectively. The mean bond length of the  $B''\text{O}_6$  octahedra decreases linearly as the Ta concentration increases, as presented in Fig. 2, indicating that the mean volume of the  $B''\text{O}_6$  octahedra declined linearly as the Ta concentration was increased. Although cation  $\text{Nb}^{5+}$  (0.67  $\text{\AA}$ ) is slightly smaller than  $\text{Ta}^{5+}$  ion (0.68  $\text{\AA}$ ) by EXAFS fitting, the large mean Nb–O bond length provides more space for  $\text{Nb}^{5+}$  ions than the Ta–O bond does for  $\text{Ta}^{5+}$  ions. Based on the above discussion, when an external electric field is applied to  $x\text{BMT} + (1-x)\text{BMN}$  ceramics, the displacement of  $\text{Nb}^{5+}$  against the oxygen cage exceeds that of  $\text{Ta}^{5+}$ . Hence, polarization the  $\text{NbO}_6^-$  caused by microwave propagation exceeds that of  $\text{TaO}_6^-$ . Consequently, the linear drop of the microwave dielectric constant as the Ta concentration increases is caused mainly by the smallness of the  $\text{TaO}_6$ .

The size homogeneity of  $B''\text{O}_6$  is another cause for why the  $Qf$  values of the BMT and BMN exceed those of the  $\text{TaO}_6$  and  $\text{NbO}_6$  mixed samples, i.e.,  $x=0.25$ ,  $x=0.5$ , and  $x=0.75$  samples. However, the smallest Ta–O bond length in the BMT sample, presented in Fig. 2, shows that the  $\text{TaO}_6$ -octahedral cages of BMT are the most rigid, and the fact that BMT has a higher  $Qf$  value than BMN is unsurprising, since denser materials are generally expected to have higher  $Qf$  values. However, the  $x=0.25$  and  $x=0.75$  samples have similar ordering characteristics, which is inconsistent with the above prediction; rather, the  $Qf$  value of the 0.75BMT+0.25BMN sample is around two and a half times smaller than that of the 0.25BMT+0.75BMN sample. Apparently, a factor other than the 1:2 ordered structure affects the microwave performance. The distortion of the oxygen octahedron is commonly considered to reduce the  $Qf$  values, although the definition of distorted oxygen octahedron is not well determined in such a case.

The deformation of the oxygen octahedral cages can be determined from the difference between the Ta–O<sup>1,2</sup> and Nb–O<sup>1,2</sup> bond lengths,  $\Delta(\text{Nb}^1, \text{Ta}^1)$ . Figure 3 plots the difference between the mean  $B''$ –O bond lengths of the first nearest oxygen atoms,  $\Delta(\text{Nb}^1, \text{Ta}^1)$ ; difference

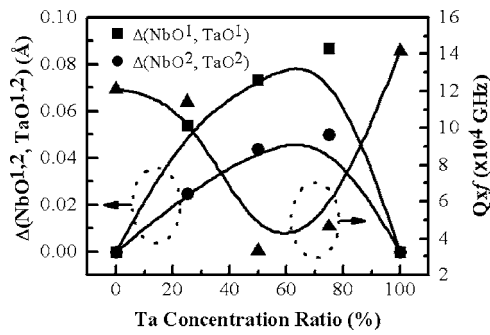


FIG. 3. Correlation of  $\Delta(\text{NbO}^{1.2}-\text{TaO}^{1.2})$  with  $Q_f$  value.

between those of the second nearest oxygen atoms in the  $\text{NbO}_6$  and  $\text{TaO}_6$  octahedra,  $\Delta(\text{Nb}-\text{O}^2, \text{Ta}-\text{O}^2)$ ; and  $Q_f$  values versus the Ta concentration.  $\Delta(\text{Nb}-\text{O}^1, \text{Ta}-\text{O}^1)$  and  $\Delta(\text{Nb}-\text{O}^2, \text{Ta}-\text{O}^2)$  for BMT and BMN samples are both zero, because only  $\text{TaO}_6$  or  $\text{NbO}_6$  is present in the BMT or BMN sample. Figure 3 shows that  $\Delta(\text{Nb}-\text{O}^1, \text{Ta}-\text{O}^1)$  is in the range of 0.05–0.09 Å and  $\Delta(\text{Nb}-\text{O}^2, \text{Ta}-\text{O}^2)$  is around 0.02–0.05 Å for the  $x=0.25, 0.5$ , and  $0.75$  samples. Both  $\Delta(\text{Nb}-\text{O}^1, \text{Ta}-\text{O}^1)$  and  $\Delta(\text{Nb}-\text{O}^2, \text{Ta}-\text{O}^2)$  for the  $0.75\text{BMT}+0.25\text{BMN}$  sample are significantly higher, and the values are about double those of the  $0.25\text{BMT}+0.75\text{BMN}$  sample. Randomly mixed  $\text{TaO}_6$  and  $\text{NbO}_6$  with large  $\Delta(\text{Nb}-\text{O}^1, \text{Ta}-\text{O}^1)$  and  $\Delta(\text{Nb}-\text{O}^2, \text{Ta}-\text{O}^2)$  clearly affects the chemical bonding among the oxygen octahedra. Therefore, the oxygen octahedra are expected to become slightly distorted and to twist, dampening the microwave propagation, and yielding low  $Q_f$  values. The  $0.75\text{BMT}+0.25\text{BMN}$  sample has a similar  $B''$ -site ordered structure like the  $0.25\text{BMT}+0.75\text{BMN}$ , but the lack of homogeneity of the sizes of the  $B''\text{O}_6$  octahedra further degrade  $Q_f$  value.

In summary, EXAFS measurements of 1:2 ordered  $x\text{BMT}+(1-x)\text{BMN}$  ceramics were made and the microwave dielectric properties explained by the structural properties of the  $B''\text{O}_6$  octahedra thus identified. The size of the  $B''\text{O}_6$  oxygen cage strongly affects the dielectric constant. The short bond length of the Ta–O causes the dielectric constant to decline, as the Ta concentration rises. The perovskite 1:2 ordered structure is responsible for the high  $Q_f$  values of the BMT and BMN ceramics. However, the nonuniformity of the sizes of the  $B''\text{O}_6$  is critical to reducing the  $Q_f$  value of

$x=0.75$  sample. The mean volume of the  $B''\text{O}_6$  octahedra strongly affects the dielectric constant of the  $x\text{BMT}+(1-x)\text{BMN}$ . However, the nonhomogeneity of the size and the distortion of the oxygen octahedra strongly degrade the  $Q_f$  value.

The authors would like to thank the National Science Council of the Republic of China, Taiwan, for financially supporting this research under Contract No. NSC 94-2112-M-003-007.

- <sup>1</sup>S. Nomura, K. Toyama, and K. Kaneta, *Jpn. J. Appl. Phys., Part 2* **21**, L642 (1982).
- <sup>2</sup>R. Guo, A. S. Shalla, and L. E. Cross, *J. Appl. Phys.* **75**, 4704 (1994).
- <sup>3</sup>R. L. Moreira, F. M. Matinaga, and A. Dias, *Appl. Phys. Lett.* **78**, 428 (2001).
- <sup>4</sup>A. Dias, V. S. T. Ciminelli, F. M. Matinaga, and R. L. Moreira, *J. Eur. Ceram. Soc.* **21**, 2739 (2001).
- <sup>5</sup>Y. Fang, A. Hu, S. Ouyang, and J. J. Oh, *J. Eur. Ceram. Soc.* **21**, 2745 (2001).
- <sup>6</sup>I. G. Siny, R. W. Tao, R. S. Katiyar, R. A. Guo, and A. S. Bhalla, *J. Phys. Chem. Solids* **59**, 181 (1998).
- <sup>7</sup>C.-T. Chia, Y.-C. Chen, H.-F. Cheng, and I.-N. Lin, *J. Appl. Phys.* **94**, 3360 (2003).
- <sup>8</sup>Y.-C. Chen, H.-Fung Cheng, H.-L. Liu, C.-T. Chia, and I.-N. Lin, *J. Appl. Phys.* **94**, 3365 (2003).
- <sup>9</sup>S. Janaswamy, G. S. Murthy, E. D. Dias, and V. R. K. Murthy, *Mater. Lett.* **55**, 414 (2002).
- <sup>10</sup>T. Nagai, T. Inuauka, and M. Sugiyama, *Jpn. J. Appl. Phys., Part 1* **31**, 3132 (1992).
- <sup>11</sup>M. Sugiyama and T. Nagai, *Jpn. J. Appl. Phys., Part 1* **32**, 4360 (1993).
- <sup>12</sup>T. Nagai, M. Sugiyama, M. Sando, and K. Niihara, *Jpn. J. Appl. Phys., Part 1* **36**, 1146 (1997).
- <sup>13</sup>T. Nagai, M. Sugiyama, M. Sando, and K. Niihara, *Jpn. J. Appl. Phys., Part 1* **35**, 5163 (1996).
- <sup>14</sup>J. J. Rehr and R. C. Albers, *Rev. Mod. Phys.* **72**, 621 (2000).
- <sup>15</sup>R. Prins and D. C. Koningsberger, *X-Ray Absorption Principles, Applications, Techniques of EXAFS, SEXAFS and XANES* (Wiley, New York, 1988), Chaps. 1 and 6.
- <sup>16</sup>I. N. Lin, C. T. Chia, H. L. Liu, H. F. Cheng, and C. C. Chi, *Jpn. J. Appl. Phys., Part 1* **41**, 6952 (2002).
- <sup>17</sup>D. Kajfez and P. Guillon, *Dielectric Resonators* (Artech House, Norwood, MA, 1986), Chap. 6.
- <sup>18</sup>A. L. Ankudinov, B. Ravel, J. J. Rehr, and S. D. Conradson, *Phys. Rev. B* **58**, 7565 (1998).
- <sup>19</sup>R. D. Shannon, *J. Appl. Phys.* **73**, 348 (1993).
- <sup>20</sup>N. W. Grimesy and R. W. Grimesz, *J. Phys.: Condens. Matter* **9**, 6737 (1997).
- <sup>21</sup>N. W. Grimesy and R. W. Grimesz, *J. Phys.: Condens. Matter* **10**, 3029 (1998).

Applied Physics Letters is copyrighted by the American Institute of Physics (AIP). Redistribution of journal material is subject to the AIP online journal license and/or AIP copyright. For more information, see <http://ojps.aip.org/aplo/aplcr.jsp>